eXPRESS Polymer Letters Vol.14, No.8 (2020) 768–779
Available online at www.expresspolymlett.com
https://doi.org/10.3144/expresspolymlett.2020.63

Processing induced segregation in PLA/TPS blends: Factors and consequences

M. Józó[1,2], *L. Cui*[1,2], *K. Bocz*[3], *B. Pukánszky*[1,2*]

[1]Laboratory of Plastics and Rubber Technology, Department of Physical Chemistry and Materials Science, Budapest University of Technology and Economics, H-1521 Budapest, P.O. Box 91, Hungary

[2]Institute of Materials and Environmental Chemistry, Chemical Research Center, H-1519 Budapest, P.O. Box 286, Hungary

[3]Department of Organic Chemistry and Technology, Budapest University of Technology and Economics, H-1521 Budapest, P.O. Box 91, Hungary

Received 6 November 2019; accepted in revised form 21 January 2020

Abstract. Poly(lactic acid) (PLA) and thermoplastic starch (TPS) blends with two different glycerol contents were prepared by injection molding. Mechanical properties were characterized by tensile and impact testing, structure by scanning electron microscopy (SEM), Fourier transform infrared (FTIR) as well as Raman spectroscopy, and water absorption was determined as a function of time. Compression-molded specimens were used as reference. The properties of the blends cover a wide range, stiffness changes from 3.3 to around 1.0 GPa, while strength from 54 to 22 MPa as TPS content increases from 0 to 50 wt%. Heterogeneous structure forms in the blends because of the weak interaction of the components. Processing conditions do not change bulk properties. Weak interactions and the large difference in the viscosity of the components lead to the formation of a skin on the surface of the specimens. The skin consists mainly of PLA, while the core contains a larger amount of TPS. The thickness of the skin depends on processing technology and conditions; it is about 18 μm for the injection-molded, while 4.5 μm for the compression-molded parts at 50 wt% TPS content. The development of the skin layer can be advantageous in some applications because it slows down water absorption considerably.

Keywords: *biopolymers, skin and core structure, interactions, mechanical properties, water absorption*

1. Introduction

In the last few decades, biopolymers came into the focus of attention. Considerable research is done on these materials, and their use in everyday practice increases continuously as well. Various numbers are published about their growth rate from 6 to 15% [1], but even the smallest is larger than the growth rate of GDP in Europe; biopolymers are obviously the polymeric materials of the future. This significant interest and growth rate have many reasons. A considerable number of biopolymers are based on natural resources while others are biodegradable. Accordingly, they answer the questions of depleting fossil fuel resources, the problems of the accumulation of plastic waste and offer a neutral carbon footprint, which is becoming more and more important aspect of environmental protection. Moreover, abundant and renewing resources are available from natural polymers, like cellulose, lignin, natural fibers, chitin, etc. and they are usually also cheap at the same time.

Besides their advantages, biopolymers also have some drawbacks. They are often sensitive to water and heat, they are difficult to process with the traditional technologies of plastic processing and the properties of the products are usually inferior to those prepared from commodity polymers. Biopolymers are often

*Corresponding author, e-mail: bpukanszky@mail.bme.hu

modified by a number of ways to overcome these drawbacks. Blending is an obvious way to combine the advantageous properties of various biopolymers and compensate for their weaknesses. Many papers have been published in the literature on the combination of PLA and wood [2–6], natural fibers [7–11] or nanocellulose [12–15], on aliphatic polyesters and starch [16–20], and on other combination of materials [21–26].

Both PLA and starch are relatively cheap and they are available in large quantities. However, the direct combination of starch powder and PLA results in an inhomogeneous material with rather poor properties [27, 28]. Plasticized, thermoplastic starch (TPS) is blended more often with PLA to obtain a more homogeneous material [29, 30]. However, the two components are immiscible and dispersed structure forms upon blending [31]. Opinions about the compatibility or interaction of the components are considerably divided, some authors claim good compatibility [32, 33], while others complete immiscibility [34]. In a previous study, we prepared two series of PLA/TPS blends and determined their structure and properties [35]. We showed that the glycerol used for the plasticization of starch stays in that phase even after blending, and by using thermodynamic considerations we proved that the interaction between the two components is rather weak. Because of weak interfacial adhesion, the properties of the blends are moderate.

The blends were prepared by compression molding in the study mentioned above [35]. We do not know anything about the behavior of the blends under practical processing conditions like extrusion or injection molding. In heterogeneous materials, various changes may occur in the structure under such conditions as the exfoliation of clays [36], the attrition of fibers [37] or the segregation of the components [21]. Segregation was observed in polymers filled with glass beads [38–40], containing an elastomer impact modifier [41], block copolymers [42, 43] or small molecular weight additives [44, 45]. Since PLA and TPS form heterogeneous blends with weak interactions between the components, structural phenomena, first of all, segregation, may occur also in them [46, 47].

Taking into account all these considerations, the goal of our work was to prepare specimens from PLA/TPS blends and determine their structure and properties. Two series of blends were prepared using TPS with different plasticizer contents. The effect of the conditions of an industrial processing technology, injection molding, on the morphology and properties of the blends was studied in detail. The possible development of special structures during processing was also checked and their effect on blend properties was determined. Specimens prepared by compression molding earlier [35] were used as a reference in the study, and the consequences of the results for practice are also mentioned in the last section of the paper.

2. Experimental

2.1. Materials

The PLA used was the Ingeo 4032D grade (M_n = 88500 g/mol and M_w/M_n = 1.8) produced by NatureWorks (Minnetonka, MN, US), which is recommended for extrusion by the producer. The polymer (<2% D isomer) has a density of 1.24 g·cm^{-3}, while its melt flow rate (MFR) is 3.9 g/10 min at 190 °C and 2.16 kg load. The corn starch used for the preparation of TPS was supplied by Hungrana Ltd., Szabadegyháza, Hungary, and its water content was 12 wt%. Glycerol with 0.5 wt% water content was obtained from Molar Chemicals Ltd., Halásztelek, Hungary and it was used for the plasticization of starch without further purification or drying. Thermoplastic starch samples containing 36 and 47 wt% glycerol (TPS36 and TPS47, respectively) were prepared and used in the experiments. The TPS content of the injection-molded PLA/TPS blends was 0, 5, 10, 15, 20, 30, 40 and 50 wt%, while the composition of the compression-molded samples changed from 0 to 100 wt% in 10 wt% steps.

2.2. Sample preparation, processing

Corn starch was dried in an oven before composite preparation (105 °C, 24 hours). The thermoplastic starch powder was prepared by dry-blending in a Henschel FM/A10 (Zeppelin Systems GmbH., Friedrichshafen, Germany) high-speed mixer at 2000 rpm. TPS was produced by processing the dry-blend on a Rheomex 3/4" single screw extruder (Haake Technik GmbH, Vreden, Germany) attached to a Haake Rheocord EU 10 V (Haake Technik GmbH, Vreden, Germany) driving unit with the temperature profile of 140–150–160–170 °C and at 60 rpm screw speed. For the preparation of the compression-molded plates, PLA and the second component were homogenized in an internal mixer (Brabender W 50 EHT, Brabender GmbH & Co. KG, Duisburg, Germany) at 190 °C and 50 rpm for 12 min. Before homogenization

poly(lactic acid) was dried in a vacuum oven (110 °C, 4 hours). Subsequently, the melt was transferred to a Fontijne SRA 100 compression molding machine (Fontijne Presses, Delft, The Netherlands) (190 °C, 5 min) to produce 1 mm thick plates for further testing.

TPS and PLA were homogenized in a Brabender DSK 42/7 twin-screw compounder (Brabender GmbH & Co. KG, Duisburg, Germany) before injection molding. Set temperatures were 170–175–180–180 °C and the speed of the screws was 30 rpm during extrusion. Standard 4 mm thick ISO 179 type tensile specimens were injection molded using a Demag IntElect 50/330-10 type all-electric injection molding machine (Sumitomo Demag, Tokyo, Japan) with the temperature profile of 180–180–185–190 °C, at 20 °C mold temperature, 1500 bar injection and 650 bar holding pressure (decreasing to 0 bar in 12 s) and 50 s cooling time.

2.3. Characterization, measurements

Mechanical properties were characterized by tensile testing using an Instron 5566 universal testing machine (Illinois Tool Works Inc, Norwood, MA, US). The gauge length was 115 mm; tensile modulus was determined at 0.5 mm/min, while properties measured at larger deformations at 5 mm/min cross-head speed. Five parallel measurements were carried out at each blend composition. Impact resistance was determined on notched Charpy type specimens (ISO 179) at 2 mm notch depth using a Ceast Resil 5.5 equipment (Illinois Tool Works Inc, Norwood, MA, USA) both in normal as well as in instrumented impact testing. The viscosity of the components was determined by oscillatory rheometry using an Anton Paar Physica MCR 301 rheometer (Anton Paar GmbH, Graz, Austria) in the plate-plate geometry from 0.1 to 600 s^{-1} frequency. The gap was 1 mm, and the temperature was maintained at 190 °C. The composition was analyzed by Fourier transform infrared spectroscopy (FTIR). Spectra were recorded using a Bruker Tensor 27A (Bruker BioSpin Corporation, Billerica, MA, US) apparatus with a Bruker Platinum ATR probe (Bruker BioSpin Corporation, Billerica, MA, US). Spectra were recorded from 4000 to 400 cm^{-1} at 2 cm^{-1} resolution with 32 scans. Raman spectra were collected using a Horiba Jobin-Yvon LabRAM system coupled with an external 785 nm diode laser source and an Olympus BX-40 optical microscope (Horiba Jobin Yvon GmbH, Unterhaching, Germany). The spectrograph was set to provide a spectral range of 350–1550 cm^{-1} with 2 cm^{-1} resolution. First, reference spectra were collected from the neat PLA and TPS materials with an objective providing a magnification of 50 using the acquisition time of 40 s and averaging 3 measured spectra at each point. Subsequently, Raman spectra were collected along the cross-section of the blends to create line maps and to determine the thickness of the PLA skin layer of the samples. All spectra were baseline corrected and normalized before multivariate evaluation in order to eliminate the intensity deviation among the measured points. The spectral concentration of the components was determined point by point by classical least squares (CLS) modeling using the reference spectra collected from neat PLA and TPS; *i.e.* each Raman spectrum of the blends taken from any location was assumed a linear combination of the two reference spectra. The structure of the blends was studied by scanning electron microscopy (SEM) using a Jeol JSM 6380 LA apparatus (Jeol USA Inc., Peabody, MA, US). Samples were broken at liquid nitrogen temperature and then a smooth surface was created by cutting the sample with a microtome. Surfaces were etched with 1 mol HCl to remove TPS particles. Water absorption was determined at 23 °C and 52% relative humidity by the measurement of the weight increase of the specimens. The desired relative humidity was achieved with a saturated solution of $Mg(NO_3)_2$.

3. Results and discussion

The results are presented in several sections. The bulk properties of the blends and the evolution of their structure as a function of composition are discussed in the first two followed by the presentation of the segregation of the components and the considerations about the reasons for this phenomenon in the subsequent two. Consequences for properties and practice are discussed in the last section of the paper.

3.1. Bulk properties

The composition dependence of the properties of PLA/TPS blends is determined by two main factors, the large difference in the macroscopic properties of the components and their weak interaction [35]. The stiffness of the blends is plotted against their TPS content in Figure 1. The effect of the first factor is clearly seen in the figure, stiffness decreases steeply and monotonously with increasing TPS content. The

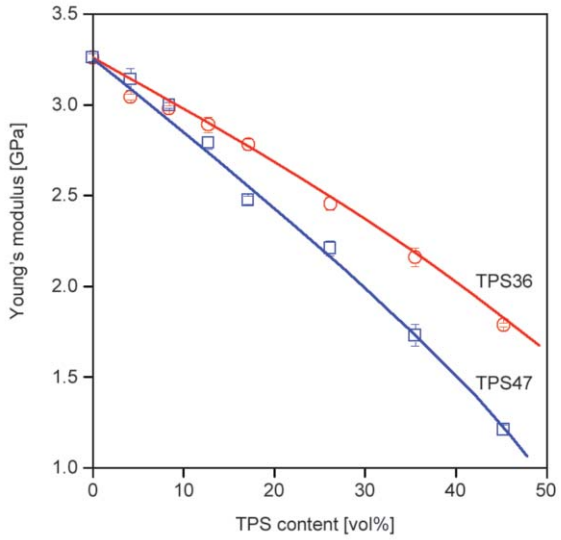

Figure 1. Young's modulus of PLA/TPS blends plotted as a function of starch (TPS) content. Effect of the degree of plasticization.
Symbols: (○) TPS36, (□) TPS47.

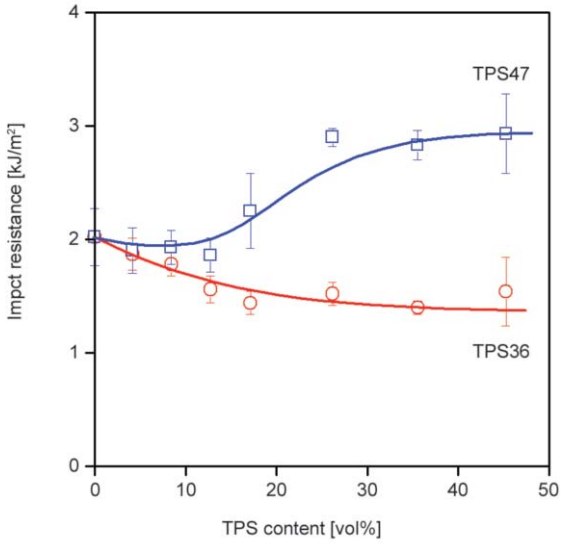

Figure 3. Dependence of the notched Charpy impact strength of PLA/TPS blends on composition.
Symbols: (○) TPS36, (□) TPS47.

effect of the second factor does not appear since stiffness is influenced only slightly by interfacial adhesion [48]. Plasticization, on the other hand, influences the inherent properties of TPS, thus Young's modulus of the blends decreases with increasing plasticizer content.

Properties measured at larger deformations, *i.e.* tensile strength and elongation-at-break in this case, show a somewhat different picture (Figure 2). Tensile strength decreases continuously with increasing TPS content, similarly to modulus, and only slight differences can be observed in the strength of the blends prepared with the two types of TPS materials, TPS36 and TPS47. The reason for this small difference is the heterogeneous structure of the blends and the weak interaction of the components. Somewhat surprisingly, the composition dependence of deformability is different for the two series of blends; elongation-at-break decreases continuously for the PLA/TPS36 blends but exhibits a maximum for the other series. Obviously, the softer particles of TPS47 and its partial solubility in the PLA matrix [35] results in the increase of deformability at intermediate TPS contents.

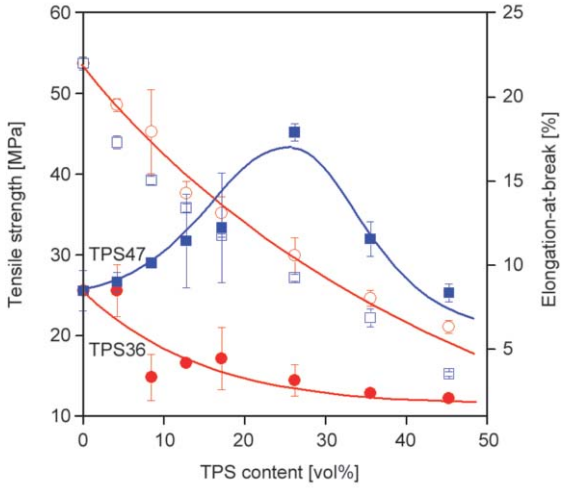

Figure 2. Effect of TPS content and the extent of plasticization on the ultimate tensile properties of PLA/TPS blends.
Symbols: (○, ●) TPS36, (□, ■) TPS47,
empty symbols: tensile strength,
full symbols: elongation-at-break.

The dissimilar deformability of the two series of blends results in different impact resistance as well. As Figure 3 shows, the impact strength of the PLA/TPS36 blends decreases continuously with increasing TPS content, while that of the PLA/TPS47 blends increases slightly above a certain TPS content, above 20 vol%. This increase is caused by the same factors mentioned above, and it could be regarded beneficial, apart from the fact that the absolute values of impact resistance are rather small; they do not exceed 3 kJ/m^2 that is not sufficient for several practical applications. We can conclude from these results that the bulk properties of the studied blends are governed by component properties, structure and the weak interaction of the components.

3.2. Structure

The heterogeneous structure of the blends has been mentioned several times in the previous section, but no evidence was supplied to support the statements.

However, previous research showed the incompatibility of the components and the development of weak interactions; thus the assumption of the formation of a heterogeneous structure seemed to be obvious. The SEM micrographs presented in Figure 4 confirm this assumption quite strongly. Voids left by dispersed TPS particles after etching are visible on the SEM micrographs shown in Figure 4a recorded on the cut surface of a specimen containing 10 wt% of the TPS47 starch. The size of the particles is rather large, in the range of 5–10 μm, which justifies the strong decrease of tensile strength with increasing TPS content (see Figure 2). The size of the particles increases somewhat with increasing TPS content as expected (Figure 4b), and some of them touch each other forming larger aggregates. The coalescence of the particles depends on their interaction with the matrix polymer and on their viscosity. The first factor facilitates, while the second hinders coalescence and the viscosity of TPS is rather large.

Structure develops further with increasing TPS content. The size of the particles increases even more and they start to form an interpenetrating network (IPN) like structure (Figure 4c). The formation of such a structure cannot be confirmed based on the presented and similar micrographs but must occur at some composition, since TPS becomes the continuous phase at large TPS content [35]. However, the composition range of the IPN structure is very narrow because of the weak interaction and poor compatibility of the components. We must also conclude that the maximum in deformability in Figure 2 is not the result of the formation of an IPN structure or phase inversion since this later occurs at larger concentration.

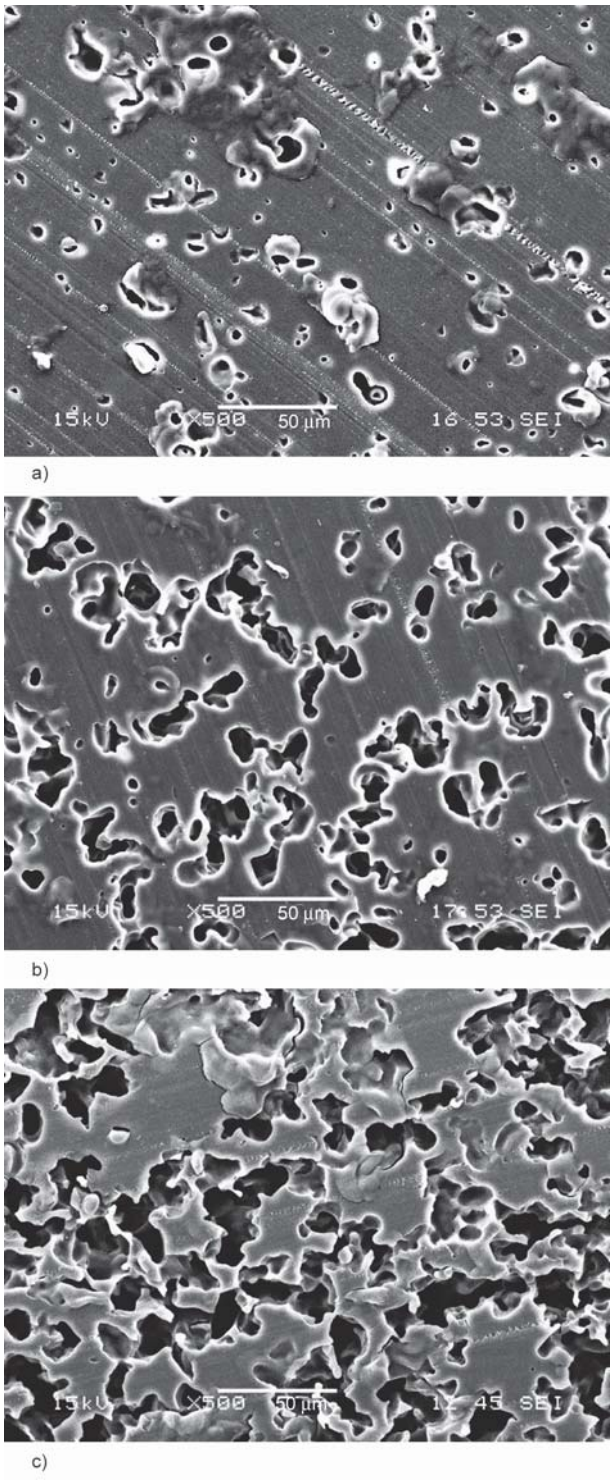

Figure 4. SEM micrographs recorded on PLA/TPS47 blends. Effect of starch content. Compression-molded specimens. TPS content: a) 10 wt%, b) 30 wt%, c) 50 wt%.

3.3. Segregation, skin formation

The micrographs presented in Figure 4 taken from compression-molded plates offered a rather uniform picture about the structure of the blends. Apart from the association of dispersed TPS particles and a hint about the formation of an IPN structure, no other structural phenomenon can be observed on them. Micrographs recorded on injection molded specimens offer a somewhat different picture as shown by Figure 5. First of all, dispersed TPS particles are elongated, they are oriented parallel to the wall of the mold. The micrographs also include the surface of the specimen and indicate the formation of a layer with a different composition from that of the core. The two micrographs presented in Figure 5 were recorded at different magnifications and both show convincingly the development of a skin layer. Moreover, Figure 5a indicates that the skin surrounds the entire specimen. The micrographs taken from the compression molded parts (Figure 4) indicate the homogeneous distribution of TPS within the specimen,

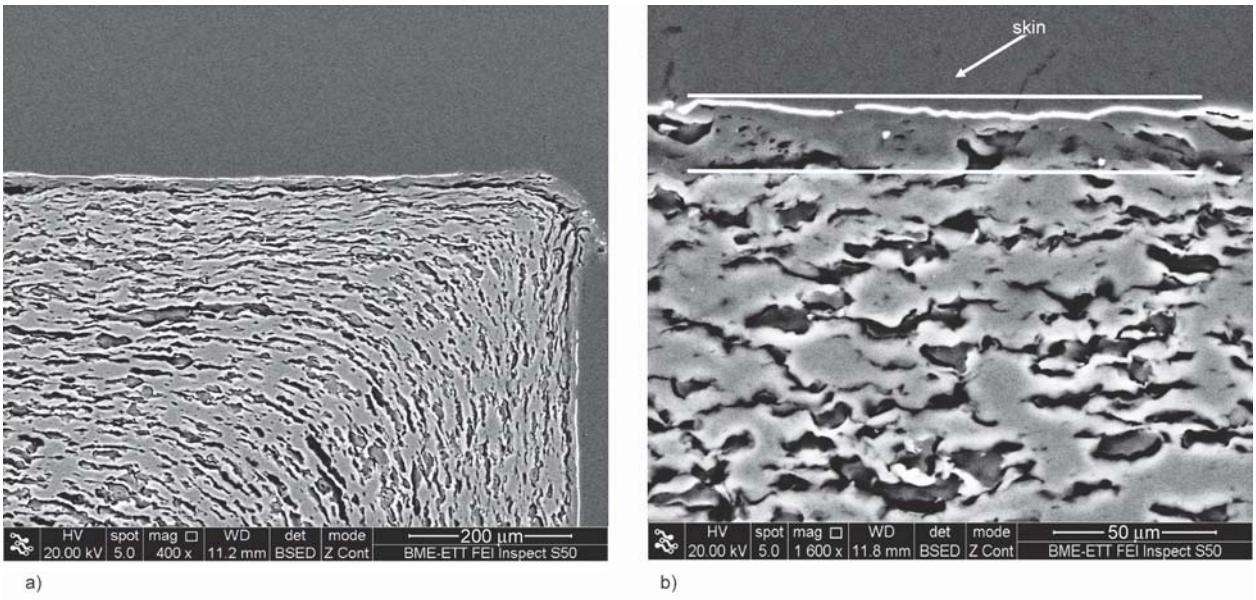

Figure 5. Structure of injection-molded PLA/TPS47 specimens. The orientation of TPS droplets and the development of a skin layer. TPS content is 50 wt%. Magnification: a) 400×, b) 1600×.

and the development of a skin layer cannot be suspected at all, at least based on those micrographs. However, closer scrutiny and investigation showed that a skin layer forms also around the compression molded plates, only its thickness is somewhat smaller than in the case of injection-molded specimens. The thickness of the skin formed is around 18 µm in injection and approximately 4.5 µm in compression molding.

FTIR spectra were recorded on the skin and the core in order to identify the main components and to determine their composition. The spectra are presented in Figure 6, together with that of the neat PLA and TPS as reference. The comparison of the spectra clearly shows that the core does not contain PLA practically at all, while the skin contains mainly PLA with a small amount of dispersed TPS. The presence of TPS is proved by the peak appearing at 1020 cm^{-1} and the broad peak around 3300 cm^{-1} both assigned to the –OH groups of starch and glycerol. The almost complete lack or a very small amount of PLA in the core is quite surprising since the micrographs in Figure 5 clearly show the continuous PLA phase, which contains dispersed TPS particles. The extinction coefficient of the ester group appearing at 1745 cm^{-1} is rather large, thus even small amounts can be detected with infrared spectroscopy. However, the band of the ester group is extremely small showing the absence or very small concentration of PLA in the core. The only explanation we can find is that the technique used, *i.e.* attenuated total reflection spectroscopy, scans only a smaller area [49] in which the TPS component dominates.

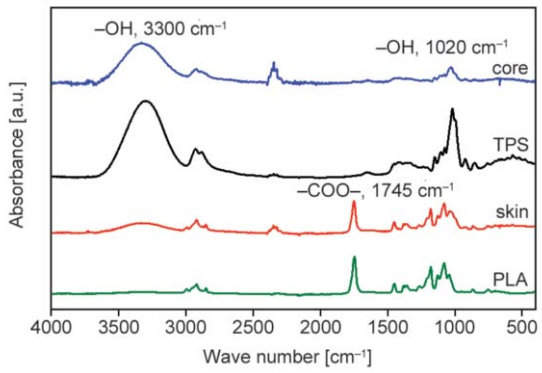

Figure 6. FTIR spectra recorded on the skin and core of injection-molded PLA/TPS47 specimens containing 50 wt% starch. The spectra of neat PLA and TPS are included as a reference. The spectra were recorded in the ATR mode.

Raman spectroscopy was also used in order to further explore the phenomenon of skin formation and characterize the composition of the layer. The spectra were taken along a line from the surface towards the core. The composition of the core and the skin is presented in Figure 7 as a function of position measured from the surface. The results confirm previous observations and indicate that the skin consists mainly of PLA, while the amount of TPS is larger in the core. The exact concentration of the two structural formations is difficult to determine because of the limitations of the measurement techniques used, as mentioned above. The explanation for the segregation

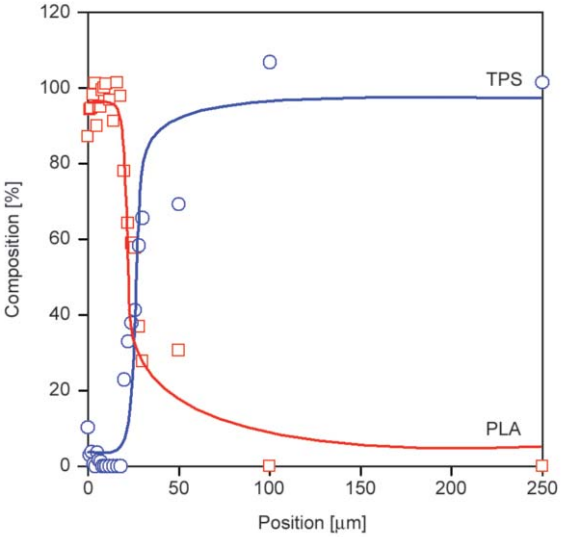

Figure 7. The composition of PLA/TPS47 blends as a function of position measured from the surface of the specimen. The composition was determined by Raman spectroscopy.

of the components and the formation of the skin and core structure needs further considerations.

3.4. Considerations, discussion

Segregation in polymeric materials containing more than one component has been observed many times. The typical phenomenon is the plate out of additives during processing or the separation of two polymers during the cleaning of an injection molding machine. Segregation has been observed in two directions, towards the center of the flow or towards the edge of the part. Segregation towards the center was observed, for example, by Szalánczi and Kubát [50], who injection molded polymers containing large glass beads to study the composition along the flow path and across it. They observed the accumulation of the beads toward the end of the part. Similarly, Karger-Kocsis and Kiss [51] observed increased elastomer content in the center of injection-molded specimens and concluded that the large difference in the viscosity of the components results in larger extent of segregation. The migration of larger molecular weight components towards the center was explained with an entropic driving force, with the larger orientation of longer molecules close to the wall of the mold [52, 53].

Migration towards the edge also occurs quite frequently. The segregation of small molecular weight components [54], additives [55, 56], block copolymers [51] and immiscible polymers [57] was also observed many times. Rezaei Kolahchi [58] used the phenomenon to modify the surface characteristics of poly(ethylene terephthalate), to improve its wettability and printability. Numerous factors determine the migration of one component during flow including surface tension [59, 60], interfacial tension towards the surface of the mold [51], the interaction of the components [18], molecular weight [61], mobility that is related to viscosity [62, 63] and determines the rate of migration.

The migration of a component during flow has been studied extensively, mostly in dilute polymer solutions. Dill and Zimm [64] developed the Equation (1) for the description of the rate of migration:

$$v = \frac{\eta_m \dot{\gamma}^2}{r k_B T} R^5 \tag{1}$$

where v is the migration velocity in the radial direction, r is the radial position, R is the chain end distance of the polymer chain in equilibrium depending on molecular weight, η_m is the viscosity of the matrix polymer, T is the temperature, k_B is Boltzman's constant and $\dot{\gamma}$ is the shear rate. The equation considers the effect of molecular weight, the viscosity of the matrix, and shear conditions but does not take into account interactions and the relative viscosity of the components although these seem to be essential factors in segregation [64, 65]. Khan *et al.* [66] assumed that the inhomogeneous stress field is the driving force, which results in migration towards smaller stresses. They assumed strong interaction among polymer molecules and thus developed Equation (2) for the rate of migration:

$$v = \frac{0.0085 \mu L^5}{kT \dot{\gamma}^2 r} \tag{2}$$

where v is the characteristic migration velocity, μ is the viscosity of the fluid, L is the half-length of the particle, r is the radial coordinate, and $\dot{\gamma}$ is the shear rate [66]. Although the authors assumed strong interactions, it does not appear in Equation (2) and they do not consider the possible effect of the viscosity ratio of the two components.

In our case, several factors must play a role in the segregation of the components. The interaction between the two components is weak; their miscibility is very limited [35]. The solubility parameters of the three components, PLA, starch and glycerol are 24.1, 26.7 and 28.9 $J^{1/2}/cm^{3/2}$, which indicates considerably larger polarity for TPS than for PLA. In accordance with the different polarity of the components, surface tensions are also different, 48.7 and 60.3 mJ/m^2 for

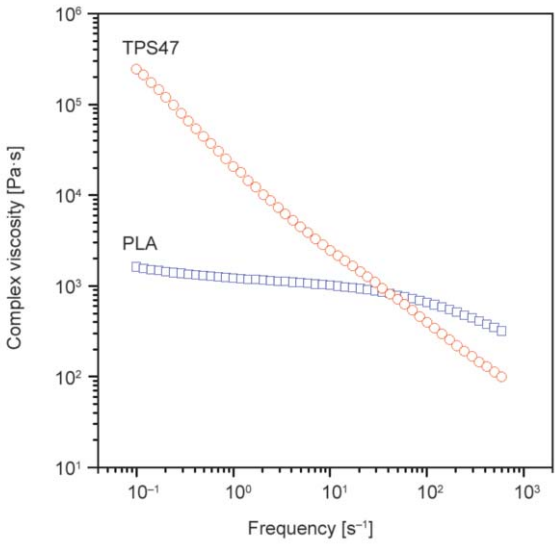

Figure 8. Frequency dependence of the complex viscosity of PLA and TPS47 determined by oscillatory rheometry in the plate-plate geometry.

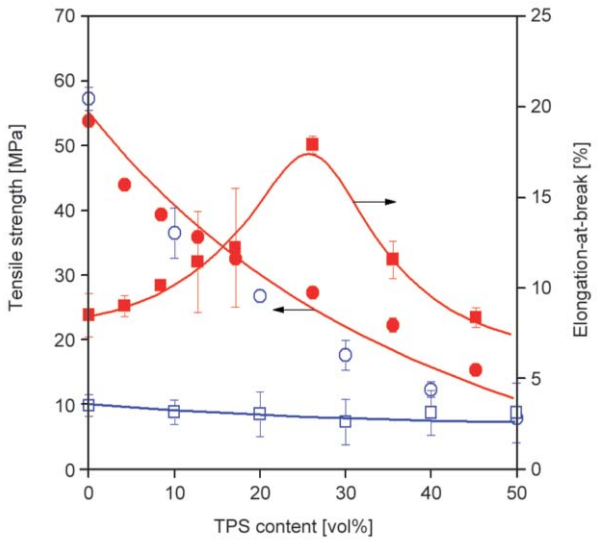

Figure 9. Comparison of the bulk properties of blend specimens prepared by compression and injection molding, respectively, from PLA/TPS47 blends. Symbols: (○, ●) tensile strength, (□, ■) elongation-at-break, empty symbols: compression-molded, full symbols: injection molded.

PLA and TPS47, respectively, favoring the migration of PLA towards the surface. The molecular weight of starch is much larger than that of PLA and also their viscosity differs considerably as shown by Figure 8, at least at small shear rates. Because of smaller molecular weight and viscosity, the mobility of PLA molecules is larger and incompatibility, as well as smaller surface tension, all drive the matrix polymer towards the surface, thus forming the skin layer. Processing conditions including different shear rates and cooling conditions, must also contribute and result in the different thickness of the skin formed in the two processing technologies, *i.e.* compression and injection molding. The formation of a skin layer and its main reasons are established, the only remaining question is the effect of this structure on blend properties.

3.5. Consequences

In order to assess the effect of the formation of the skin layer in PLA/TPS blends, first, the properties of compression and injection molded specimens are compared to each other. Although compression molded parts also develop a skin layer, its thickness is much smaller than for injection-molded specimens. The tensile strength and deformability of the two kinds of samples are compared to each other in Figure 9. Processing technology, thickness (compression-molded: 1 mm, injection-molded: 4 mm) and skin layer do not have any effect on strength. Deformability, on the other hand, is larger for the injection-molded specimen than for the compression-molded one. The difference evidently does not result from the thickness of the skin, but from the orientation of the components resulting from the mold filling process (see Figure 5). We can conclude from these, and from other results not shown, that bulk properties are not influenced much by segregation and skin formation much.

Starch, and TPS even more, is very sensitive to water. They absorb a considerable amount of water, which modifies, usually deteriorates their properties. One of the main benefits of blending is the decrease in water uptake. The relative weight increase, *i.e.* water uptake, of compression and injection molded blend samples are compared in Figure 10. The figure clearly indicates and calculations proved that equilibrium water uptake is the same for the two types of blends, but the rate of absorption differs considerably. Equilibrium water uptake is determined by the composition of the blends, by the amount of TPS, while the rate of absorption is considerably influenced by the presence of the skin. Water uptake was modeled to express these relationships quantitatively. The following form of Fick's law was fitted to the experimental points to determine the overall rate of absorption (see Equation (3)):

$$M_t = M_\infty \left\{1 - \frac{8}{\pi^2}\left[\exp(-at) + \frac{1}{9}\exp(-9at) + \frac{1}{25}\exp(-25at)\right]\right\} \quad (3)$$

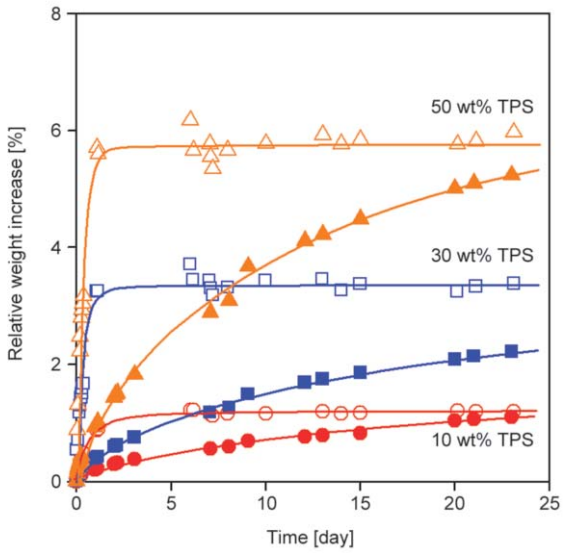

Figure 10. Water absorption isotherms of PLA/TPS47 blends of various compositions. Effect of starch (TPS) content.
Symbols: (○, ●) 10 wt%, (□, ■) 30 wt%, (△, ▲) 50 wt% TPS content; open symbols: compression molded, full symbols: injection molded.

where M_t and M_∞ are the amount of absorbed water at time t and at infinite time, respectively, and a is the overall rate of absorption. The determined rates are plotted against TPS content in Figure 11. The rate of water uptake is much smaller for the injection molded parts than for their compression-molded counterparts. The result has considerable practical consequences. Slower water uptake changes the properties of the product and modifies its lifetime. In the case of products with a determined or limited lifetime, this difference can be of practical relevance.

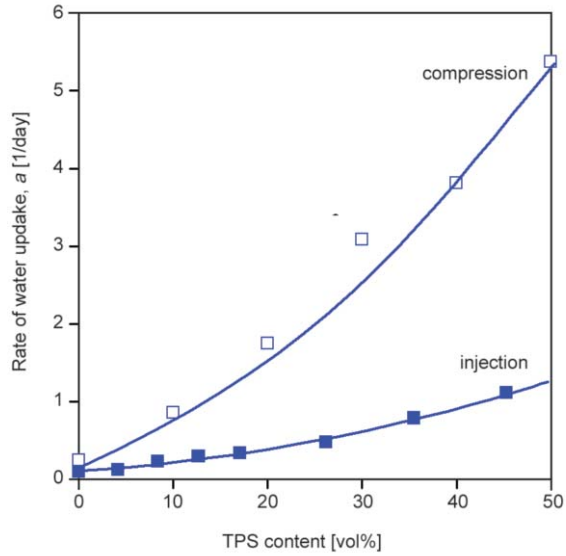

Figure 11. Effect of TPS content and processing technology on the rate of water absorption in PLA/TPS47 blends.
Symbols: (□) compression molded, (■) injection molded.

4. Conclusions

The study of PLA/TPS blend samples prepared by injection molding showed that their properties cover a wide range depending on composition. The stiffness of the blends changed from 3.3 to around 1.0 GPa and their strength from 54 to 22 MPa as TPS content increased from 0 to 50 wt%. The blends have heterogeneous structures because of the weak interaction of the components, and phase inversion cannot be observed in the studied composition range. Processing conditions do not change bulk properties, the mechanical properties of compression and injection molded parts were very similar. Weak interactions and the large difference in the viscosity of the components leads to segregation, to the formation of a skin layer on the surface of the specimens. The skin consists of mainly PLA, while the core contains a larger amount of TPS. The thickness of the skin depends on processing technology and conditions; it is about 18 μm for the injection-molded, while 4.5 μm for the compression-molded parts at 50 wt% TPS content. The development of the skin layer can be advantageous in some applications because it slows down water absorption considerably. Bulk properties must be improved for practical applications by the modification of interactions, by coupling, for example.

Acknowledgements

The significant help of Péter Müller, József Bere, and Erika Fekete Bódiné in sample preparation and measurements is highly appreciated. The authors acknowledge the financial support of the National Scientific Research Fund of Hungary (OTKA Grant No. K 120039 and FK 129270) for this project on the modification of polymeric materials.

References

[1] Dawande R.: Bioplastics market by type (biodegradable plastic and non-biodegradable plastic) and application (rigid packaging, flexible packaging, textile, agriculture & horticulture, consumer good, automotive, electronic, building & construction, and others) – Global opportunity analysis and industry forecast, 2018–2024. Allied Market Research, Portland (2017).

[2] Csikós Á., Faludi G., Domján A., Renner K., Móczó J., Pukánszky B.: Modification of interfacial adhesion with a functionalized polymer in PLA/wood composites. European Polymer Journal, **68**, 592–600 (2015). https://doi.org/10.1016/j.eurpolymj.2015.03.032

[3] Faludi G., Dóra G., Renner K., Móczó J., Pukánszky B.: Improving interfacial adhesion in PLA/wood biocomposites. Composites Science and Technology, **89**, 77–82 (2013). https://doi.org/10.1016/j.compscitech.2013.09.009

[4] Csizmadia R., Faludi G., Renner K., Móczó J., Pukánszky B.: PLA/wood biocomposites: Improving composite strength by the chemical treatment of the fibers. Composites Part A: Applied Science and Manufacturing, **53**, 46–53 (2013). https://doi.org/10.1016/j.compositesa.2013.06.003

[5] Ecker J. V., Haider A., Burzic I., Huber A., Eder G., Hild S.: Mechanical properties and water absorption behaviour of PLA and PLA/wood composites prepared by 3D printing and injection moulding. Rapid Prototyping Journal, **25**, 672–678 (2019). https://doi.org/10.1108/RPJ-06-2018-0149

[6] Dong Y., Milentis J., Pramanik A.: Additive manufacturing of mechanical testing samples based on virgin poly (lactic acid) (PLA) and PLA/wood fibre composites. Advances in Manufacturing, **6**, 71–82 (2018). https://doi.org/10.1007/s40436-018-0211-3

[7] Mazzanti V., Pariante R., Bonanno A., de Ballesteros O. R., Mollica F., Filippone G.: Reinforcing mechanisms of natural fibers in green composites: Role of fibers morphology in a PLA/hemp model system. Composites Science and Technology, **180**, 51–59 (2019). https://doi.org/10.1016/j.compscitech.2019.05.015

[8] Gunti R., Ratna Prasad A. V., Gupta A. V. S. S. K. S.: Mechanical and degradation properties of natural fiber-reinforced PLA composites: Jute, sisal, and elephant grass. Polymer Composites, **39**, 1125–1136 (2018). https://doi.org/10.1002/pc.24041

[9] Siakeng R., Jawaid M., Ariffin H., Sapuan S. M., Asim M., Saba N.: Natural fiber reinforced polylactic acid composites: A review. Polymer Composites, **40**, 446–463 (2019). https://doi.org/10.1002/pc.24747

[10] Scaffaro R., Lopresti F., Botta L.: PLA based biocomposites reinforced with *Posidonia oceanica* leaves. Composites Part B: Engineering, **139**, 1–11 (2018). https://doi.org/10.1016/j.compositesb.2017.11.048

[11] Li X., Hegyesi N., Zhang Y., Mao Z., Feng X., Wang B., Pukánszky B., Sui X.: Poly(lactic acid)/lignin blends prepared with the Pickering emulsion template method. European Polymer Journal, **110**, 378–384 (2019). https://doi.org/10.1016/j.eurpolymj.2018.12.001

[12] Ghasemi S., Behrooz R., Ghasemi I., Yassar R. S., Long F.: Development of nanocellulose-reinforced PLA nanocomposite by using maleated PLA (PLA-*g*-MA). Journal of Thermoplastic Composite Materials, **31**, 1090–1101 (2018). https://doi.org/10.1177/0892705717734600

[13] Kian L. K., Saba N., Jawaid M., Sultan M. T. H.: A review on processing techniques of bast fibers nanocellulose and its polylactic acid (PLA) nanocomposites. International Journal of Biological Macromolecules, **121**, 1314–1328 (2019). https://doi.org/10.1016/j.ijbiomac.2018.09.040

[14] Zhang Y., Cui L., Xu H., Feng X., Wang B., Pukánszky B., Mao Z., Sui X.: Poly(lactic acid)/cellulose nanocrystal composites *via* the Pickering emulsion approach: Rheological, thermal and mechanical properties. International Journal of Biological Macromolecules, **137**, 197–204 (2019). https://doi.org/10.1016/j.ijbiomac.2019.06.204

[15] Hegyesi N., Zhang Y., Kohári A., Polyák P., Sui X., Pukánszky B.: Enzymatic degradation of PLA/cellulose nanocrystal composites. Industrial Crops and Products, **141**, 111799/1-111799/8 (2019). https://doi.org/10.1016/j.indcrop.2019.111799

[16] Soares F. C., Yamashita F., Müller C. M. O., Pires A. T. N.: Effect of cooling and coating on thermoplastic starch/poly(lactic acid) blend sheets. Polymer Testing, **33**, 34–39 (2014). https://doi.org/10.1016/j.polymertesting.2013.11.001

[17] Li H., Huneault M. A.: Comparison of sorbitol and glycerol as plasticizers for thermoplastic starch in TPS/PLA blends. Journal of Applied Polymer Science, **119**, 2439–2448 (2011). https://doi.org/10.1002/app.32956

[18] Koh J. J., Zhang X., Kong J., He C.: Compatibilization of multicomponent composites through a transitioning phase: Interfacial tensions considerations. Composites Science and Technology, **164**, 34–43 (2018). https://doi.org/10.1016/j.compscitech.2018.05.030

[19] Yokesahachart C., Yoksan R.: Effect of amphiphilic molecules on characteristics and tensile properties of thermoplastic starch and its blends with poly(lactic acid). Carbohydrate Polymers, **83**, 22–31 (2011). https://doi.org/10.1016/j.carbpol.2010.07.020

[20] Móczó J., Kun D., Fekete E.: Desiccant effect of starch in polylactic acid composites. Express Polymer Letters, **12**, 1014–1024 (2018). https://doi.org/10.3144/expresspolymlett.2018.88

[21] Sui G., Jing M., Zhao J., Wang K., Zhang Q., Fu Q.: A comparison study of high shear force and compatibilizer on the phase morphologies and properties of polypropylene/polylactide (PP/PLA) blends. Polymer, **154**, 119–127 (2018). https://doi.org/10.1016/j.polymer.2018.09.005

[22] Arrieta M. P., Fortunati E., Dominici F., López J., Kenny J. M.: Bionanocomposite films based on plasticized PLA–PHB/cellulose nanocrystal blends. Carbohydrate Polymers, **121**, 265–275 (2015). https://doi.org/10.1016/j.carbpol.2014.12.056

[23] Zembouai I., Kaci M., Bruzaud S., Dumazert L., Bourmaud A., Mahlous M., Lopez-Cuesta J. M., Grohens Y.: Gamma irradiation effects on morphology and properties of PHBV/PLA blends in presence of compatibilizer and Cloisite 30B. Polymer Testing, **49**, 29–37 (2016). https://doi.org/10.1016/j.polymertesting.2015.11.003

[24] Arruda L. C., Magaton M., Bretas R. E. S., Ueki M. M.: Influence of chain extender on mechanical, thermal and morphological properties of blown films of PLA/PBAT blends. Polymer Testing, **43**, 27–37 (2015). https://doi.org/10.1016/j.polymertesting.2015.02.005

[25] de Lucas-Freile A., Sancho-Querol S., Yánez-Pacios A. J., Marín-Perales L., Martín-Martínez J. M.: Blends of ethylene-*co*-vinyl acetate and poly(3-hydroxybutyrate) with adhesion property. Express Polymer Letters, **12**, 600–615 (2018). https://doi.org/10.3144/expresspolymlett.2018.51

[26] Cailloux J., Abt T., García-Masabet V., Santana O., Sánchez-Soto M., Carrasco F., Maspoch M. L.: Effect of the viscosity ratio on the PLA/PA10.10 bioblends morphology and mechanical properties. Express Polymer Letters, **12**, 569–582 (2018). https://doi.org/10.3144/expresspolymlett.2018.47

[27] Jun C. L.: Reactive blending of biodegradable polymers: PLA and starch. Journal of Polymers and Environment, **8**, 33–37 (2000). https://doi.org/10.1023/A:1010172112118

[28] Jang W. Y., Shin B. Y., Lee T. J., Narayan R.: Thermal properties and morphology of biodegradable PLA/starch compatibilized blends. Journal of Industrial and Engineering Chemistry, **13**, 457–464 (2007).

[29] Akrami M., Ghasemi I., Azizi H., Karrabi M., Seyedabadi M.: A new approach in compatibilization of the poly(lactic acid)/thermoplastic starch (PLA/TPS) blends. Carbohydrate Polymers, **144**, 254–262 (2016). https://doi.org/10.1016/j.carbpol.2016.02.035

[30] Li H., Huneault M. A.: Crystallization of PLA/thermoplastic starch blends. International Polymer Processing, **23**, 412–418 (2008). https://doi.org/10.3139/217.2185

[31] Martin O., Avérous L.: Poly(lactic acid): Plasticization and properties of biodegradable multiphase systems. Polymer, **42**, 6209–6219 (2001). https://doi.org/10.1016/S0032-3861(01)00086-6

[32] Wang N., Yu J., Chang P. R., Ma X.: Influence of formamide and water on the properties of thermoplastic starch/poly(lactic acid) blends. Carbohydrate Polymers, **71**, 109–118 (2008). https://doi.org/10.1016/j.carbpol.2007.05.025

[33] Wang N., Yu J., Ma X.: Preparation and characterization of compatible thermoplastic dry starch/poly(lactic acid). Polymer Composites, **29**, 551–559 (2008). https://doi.org/10.1002/pc.20399

[34] Mittal V., Akhtar T., Luckachan G., Matsko N.: PLA, TPS and PCL binary and ternary blends: Structural characterization and time-dependent morphological changes. Colloid and Polymer Science, **293**, 573–585 (2015). https://doi.org/10.1007/s00396-014-3458-7

[35] Müller P., Bere J., Fekete E., Móczó J., Nagy B., Kállay M., Gyarmati B., Pukánszky B.: Interactions, structure and properties in PLA/plasticized starch blends. Polymer, **103**, 9–18 (2016). https://doi.org/10.1016/j.polymer.2016.09.031

[36] Rajesh J. J., Soulestin J., Lacrampe M. F., Krawczak P.: Effect of injection molding parameters on nanofillers dispersion in masterbatch based PP-clay nanocomposites. Express Polymer Letters, **6**, 237–243 (2012). https://doi.org/10.3144/expresspolymlett.2012.26

[37] Bailey R., Kraft H.: A study of fibre attrition in the processing of long fibre reinforced thermoplastics. International Polymer Processing, **2**, 94–101 (1987). https://doi.org/10.3139/217.870094

[38] Molina-Boisseau S., le Bolay N.: The mixing of a polymeric powder and the grinding medium in a shaker bead mill. Powder Technology, **123**, 212–220 (2002). https://doi.org/10.1016/S0032-5910(01)00460-0

[39] Kovács J. G.: Shrinkage alteration induced by segregation of glass beads in injection molded PA6: Experimental analysis and modeling. Polymer Engineering and Science, **51**, 2517–2525 (2011). https://doi.org/10.1002/pen.22025

[40] Balke S. T., Hu J., Joseph S., Karami A., Salerni R., Planeta M., Suhay J., Tamber H.: Polymer and particle separation during extrusion. in 'Proceeding of Annual Technical Conference for Plastics Professionals. Atlanta, USA', Vol 1, 205–211 (1998).

[41] Yamashita T., Nabeshima Y.: A study of the microscopic plastic deformation process in poly(methylmethacrylate)/acrylic impact modifier compounds by means of small angle X-ray scattering. Polymer, **41**, 6067–6079 (2000). https://doi.org/10.1016/S0032-3861(99)00856-3

[42] Yan X., Liu G., Li Z.: Preparation and phase segregation of block copolymer nanotube multiblocks. Journal of the American Chemical Society, **126**, 10059–10066 (2004). https://doi.org/10.1021/ja0479890

[43] Fukuhara K., Fujii Y., Nagashima Y., Hara M., Nagano S., Seki T.: Liquid-crystalline polymer and block copolymer domain alignment controlled by free-surface segregation. Angewandte Chemie, **52**, 5988–5991 (2013). https://doi.org/10.1002/anie.201300560

[44] Bhattacharyya S. K., De S. K., Basu S.: Studies on poly(vinyl chloride)-copper composites. Part 1: State of segregation of filler particles, electrical and mechanical properties in presence of plasticizer and stabilizer. Polymer Engineering and Science, **19**, 533–539 (1979). https://doi.org/10.1002/pen.760190802

[45] Briddick A., Li P., Hughes A., Courchay F., Martinez A., Thompson R. L.: Surfactant and plasticizer segregation in thin poly(vinyl alcohol) films. Langmuir, **32**, 864–872 (2016). https://doi.org/10.1021/acs.langmuir.5b03758

[46] Lourdin D., Coignard L., Bizot H., Colonna P.: Influence of equilibrium relative humidity and plasticizer concentration on the water content and glass transition of starch materials. Polymer, **38**, 5401–5406 (1997). https://doi.org/10.1016/S0032-3861(97)00082-7

[47] Vikman M., Hulleman S. H. D., van der Zee M., Myllärinen P., Feil H.: Morphology and enzymatic degradation of thermoplastic starch–polycaprolactone blends. Journal of Applied Polymer Science, **74**, 2594–2604 (1999). https://doi.org/10.1002/(SICI)1097-4628(19991209)74:11<2594::AID-APP5>3.0.CO;2-R

[48] Gupta V. B., Mittal R. K., Sharma P. K., Mennig G., Wolters J.: Some studies on glass fiber-reinforced polypropylene. Part II: Mechanical properties and their dependence on fiber length, interfacial adhesion, and fiber dispersion. Polymer Composites, **10**, 16–27 (1989). https://doi.org/10.1002/pc.750100104

[49] Kazarian S. G., Chan K. L. A.: ATR-FTIR spectroscopic imaging: Recent advances and applications to biological systems. Analyst, **138**, 1940–1951 (2013). https://doi.org/10.1039/C3AN36865C

[50] Kubát J., Szalánczi Á.: Polymer-glass separation in the spiral mold test. Polymer Engineering and Science, **14**, 873–877 (1974). https://doi.org/10.1002/pen.760141211

[51] Karger-Kocsis J., Kiss L.: Dynamic mechanical properties and morphology of polypropylene block copolymers and polypropylene/elastomer blends. Polymer Engineering and Science, **27**, 254–262 (1987). https://doi.org/10.1002/pen.760270404

[52] Breuer O., Tchoudakov R., Narkis M., Siegmann A.: Segregated structures in carbon black-containing immiscible polymer blends: HIPS/LLDPE systems. Journal of Applied Polymer Science, **64**, 1097–1106 (1997). https://doi.org/10.1002/(SICI)1097-4628(19970509)64:6<1097::AID-APP9>3.0.CO;2-G

[53] Miccio L. A., Liaño R., Schreiner W. H., Montemartini P. E., Oyanguren P. A.: Partially fluorinated polymer networks: Surface and tribological properties. Polymer, **51**, 6219–6226 (2010). https://doi.org/10.1016/j.polymer.2010.10.036

[54] Chen Z., Ward R., Tian Y., Eppler A. S., Shen Y. R., Somorjai G. A.: Surface composition of biopolymer blends biospan-SP/phenoxy and biospan-F/phenoxy observed with SFG, XPS, and contact angle goniometry. The Journal of Physical Chemistry B, **103**, 2935–2942 (1999). https://doi.org/10.1021/jp984502z

[55] Lee H., Arher L. A.: Functionalizing polymer surfaces by field-induced migration of copolymer additives. 1. Role of surface energy gradients. Macromolecules, **34**, 4572–4579 (2001). https://doi.org/10.1021/ma001278e

[56] Lee H., Archer L. A.: Functionalizing polymer surfaces by surface migration of copolymer additives: Role of additive molecular weight. Polymer, **43**, 2721–2728 (2002). https://doi.org/10.1016/S0032-3861(02)00041-1

[57] Qian H., Zhang Y. X., Huang S. M., Lin Z. Y.: Effect of the surface-modifying macromolecules on the duration of the surface functionalization. Applied Surface Science, **253**, 4659–4667 (2007). https://doi.org/10.1016/j.apsusc.2006.10.017

[58] Rezaei Kolahchi A., Ajji A., Carreau P. J.: Enhancing hydrophilicity of polyethylene terephthalate surface through melt blending. Polymer Engineering and Science, **55**, 349–358 (2015). https://doi.org/10.1002/pen.23910

[59] You J., Liao Y., Men Y., Shi T., An L., Li X.: Composition effect on interplay between phase separation and dewetting in PMMA/SAN blend ultrathin films. Macromolecules, **44**, 5318–5325 (2011). https://doi.org/10.1021/ma200082m

[60] Cheung Z-L., Weng L-T., Chan C-M., Hou W. M., Li L.: Morphology-driven surface segregation in a blend of poly(ε-caprolactone) and poly(vinyl chloride). Langmuir, **21**, 7968–7970 (2005). https://doi.org/10.1021/la050649n

[61] Chen H-L., Li L-J., Lin T-L.: Formation of segregation morphology in crystalline/amorphous polymer blends: Molecular weight effect. Macromolecules, **31**, 2255–(1998). https://doi.org/10.1021/ma9715740

[62] Reignier J., Favis B. D.: Core–shell structure and segregation effects in composite droplet polymer blends. AlChE Journal, **49**, 1014–1023 (2003). https://doi.org/10.1002/aic.690490418

[63] Fourati Y., Tarrés Q., Mutjé P., Boufi S.: PBAT/thermoplastic starch blends: Effect of compatibilizers on the rheological, mechanical and morphological properties. Carbohydrate Polymers, **199**, 51–57 (2018). https://doi.org/10.1016/j.carbpol.2018.07.008

[64] Dill K. A., Zimm B. H.: A rhelogical separator for very large DNA molecules. Nucleic Acids Research, **7**, 735–749 (1979). https://doi.org/10.1093/nar/7.3.735

[65] MacDonald M. J., Muller S. J.: Experimental study of shear-induced migration of polymers in dilute solutions. Journal of Rheology, **40**, 259–283 (1996). https://doi.org/10.1122/1.550740

[66] Khan M. B., Briscoe B. J., Richardson M.: Field-induced phase fractionation in multiphase polymer flow systems: A review. Polymer-Plastics Technology and Engineering, **33**, 295–322 (1994). https://doi.org/10.1080/03602559408013095